Current Biology 24, 1615–1619, July 21, 2014 ©2014 Elsevier Ltd All rights reserved http://dx.doi.org/10.1016/j.cub.2014.05.056

Report

A Specialized Bird Pollination System with a Bellows Mechanism for Pollen Transfer and Staminal Food Body Rewards

Agnes S. Dellinger,[1,*] Darin S. Penneys,[2] Yannick M. Staedler,[1] Lena Fragner,[3] Wolfram Weckwerth,[3] and Jürg Schönenberger[1,*]

[1]Department of Botany and Biodiversity Research, Faculty of Life Sciences, University of Vienna, Rennweg 14, 1030 Vienna, Austria

[2]Department of Botany, California Academy of Sciences, Golden Gate Park, 55 Music Concourse Drive, San Francisco, CA 94118, USA

[3]Department of Ecogenomics and Systems Biology, Faculty of Life Sciences, University of Vienna, Althanstrasse 14, 1090 Vienna, Austria

Summary

Bird pollination has evolved repeatedly among flowering plants but is almost exclusively characterized by passive transfer of pollen onto the bird and by nectar as primary reward [1, 2]. Food body rewards are exceedingly rare among eudicot flowering plants and are only known to occur on sterile floral organs [3]. In this study, we report an alternative bird pollination mechanism involving bulbous stamen appendages in the Neotropical genus *Axinaea* (Melastomataceae). We studied the pollination process by combining pollination experiments, video monitoring, and detailed analyses of stamen structure and metabolomic composition. We show that the bulbous stamen appendages, which are consumed by various species of passerines (Thraupidae, Fringillidae), are bifunctional during the pollination process. First, the appendages work as bellows organs in a unique pollen expulsion mechanism activated by the passerines. As the birds seize an appendage with their beaks in order to remove it from the flower for consumption, air contained in the appendage's aerenchymatous tissue is pressed into the hollow anther. The resulting air flow causes the expulsion of a pollen jet and the deposition of pollen on the bird's head and beak. Second, the stamen appendages provide a hexose-rich, highly nutritious (15,100 J/g) food body reward for the pollinating passerines. This discovery expands our knowledge of flowering plant pollination systems and provides the first report of highly specialized bellows organs for active pollen transfer in flowering plants. In addition, this is the only known case of a food body reward associated with reproductive structures in the eudicot clade of flowering plants.

Results

General Floral Morphology of *Axinaea*

The flowers of the five *Axinaea* species studied here are weakly monosymmetric and usually pentamerous, with two whorls of five fertile stamens each, borne on a short hypanthium (Figures 1A–1C). On each stamen, a conspicuous, sterile, bulbous appendage derived from connective tissue is present. The androecium, and particularly the anther appendages, display a strong color contrast with respect to the corolla (Figures 1A and 1B; Figure S1 available online). The stamens are inflexed in the region of the joint between anther and filament so that the tip of the anther is positioned close to the base of the filament (Figures 1C and 1D; Figure 2A; less pronounced in *Axinaea affinis*, Figure S1A). The style is curved downward in the horizontally oriented flowers (Figures 1A, 1B, S1A, and S1D). In *Axinaea confusa*, *Axinaea costaricensis*, and *Axinaea macrophylla*, the corolla remains erect and partly covers the stamens during anthesis, whereas it opens wider in *Axinaea affinis* and *Axinaea sclerophylla*, exposing the stamens more clearly. The distal-most part of the style with the stigma is exserted from the corolla in all species (Figures 1A–1C and S1D), sometimes even prior to anthesis.

Pollinator Observations and Mating System Experiments

We observed different species of passerines visiting flowers of *Axinaea* species (Table 1; Movies S1 and S2). Sporadic insect visitors (Curculionidae, Elateridae, Heteroptera) did not display any foraging behavior, and no bees were observed on the flowers.

Using their beaks, the perching birds seized a bulbous stamen appendage, ripped it from the flower, and consumed the appendage together with the anther and part of the filament (Figures 1G, 1H, S1B, and S1D). We observed that upon initially seizing and compressing the appendage, a pollen jet was ejected from the terminal anther pore (Movie S1), coating the bird's beak, forehead, or neck (Figure 1H). The birds usually removed the stamens one by one and did not discriminate between the two stamen whorls. Over the course of anthesis (flowers open shortly before sunrise and are anthetic for up to 9 days in *A. confusa*), the initial ten stamens are removed continuously until none remain (Figures 1E and 1F). Fifty-four percent of the flowers were visited on at least 2 different days until complete stamen removal.

Our mating system experiments indicate that *A. confusa* is mostly outcrossing (Table 2), but not pollen limited, and self-compatible (self-compatibility index of 1.14). There was no apomictic fruit set, and fruit set in the autogamy trial was very low (Table 2). Pollen ejected from the stamens by artificial activation of the bellows mechanism can reach the stigma of the same flower, but fruit set is lower (32 fruits out of 90 flowers) than when naturally pollinated ($X^2 = 23.26$, degrees of freedom = 2, $p = 8.9 \times 10^{-0.6}$).

Stamen Structure of *Axinaea*

High-resolution X-ray computed tomographic (HRXCT) and light microscopic analyses revealed that the bulbous appendages are composed of aerenchymatous tissue with extremely loosely arranged cells and high proportions of intercellular space (Figures 2C and 2D; Movie S3). The proportion of intercellular space in the appendages of *A. confusa*, as calculated via volumetric measurements on a high-resolution 3D tomography model, amounts to 38% of the total volume of the appendage. Importantly, in mature anthers, there are no distinct cell layers separating the aerenchymatous tissue of

*Correspondence: agnes.dellinger@univie.ac.at (A.S.D.), juerg.schoenenberger@univie.ac.at (J.S.)

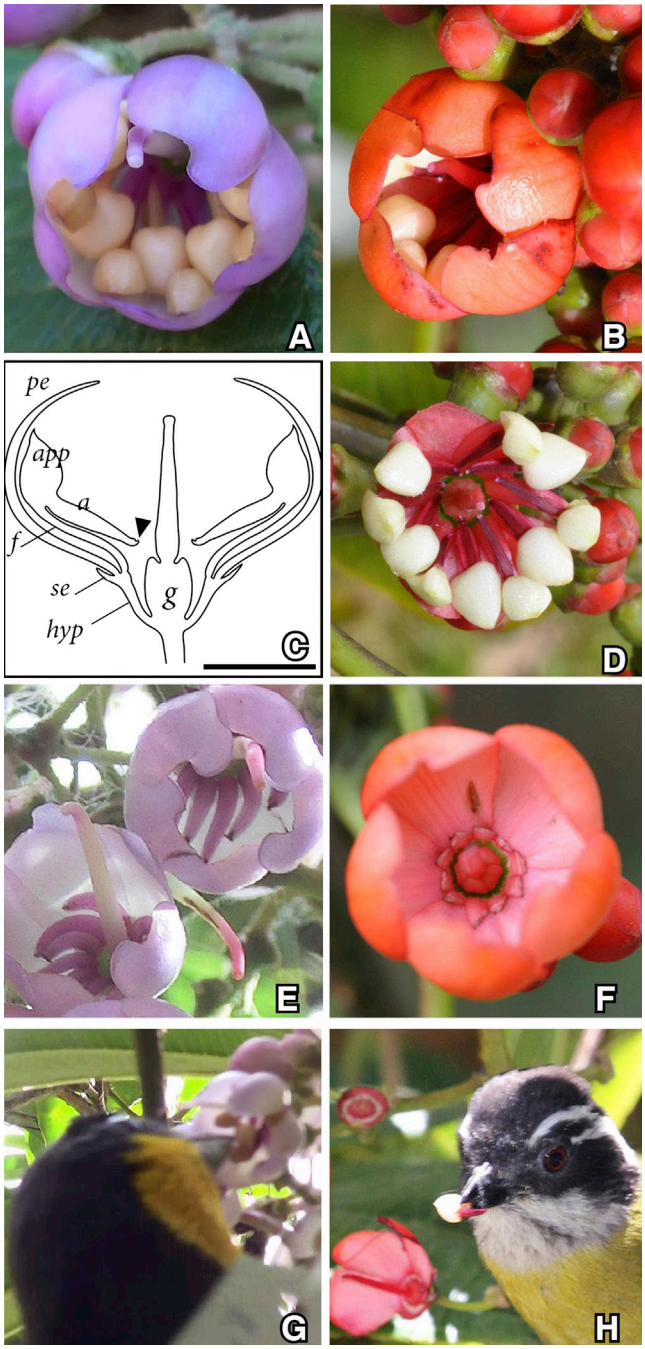

Figure 1. Flowers of *Axinaea* and Pollinating Tanagers

(A and B) Intact, virgin flowers of *Axinaea*.

(A) *Axinaea confusa*.

(B) *Axinaea costaricensis*.

(C) Half-schematic line drawing showing a longitudinal section of an anthetic flower of *A. confusa*. Arrowhead indicates thecal pore in one of the anthers. The scale bar represents 0.5 cm.

(D) Virgin flower of *A. costaricensis*, with petals partly removed manually to expose the stamens. Note that anther arrangement is not polysymmetric but is weighted toward the lower (abaxial) side of the horizontally oriented flower (compare with Figures S1A and S1B).

(E and F) Flowers after pollinator visitation and stamen removal.

(E) *A. confusa*. Note that entire filaments remain in the flower and that the filaments of antepetalous stamens are significantly longer than those of antesepalous stamens.

(F) *A. costaricensis*. Note that only the proximal-most parts of filaments remain.

the appendage from the two pollen chambers (Figures 2C, 2E, 2F, and S2B), thus there is a direct connection between pollen chambers and appendage. In the remainder of the anther, the connective tissue is separated from the pollen chambers by distinct cell layers (Figures 2B and S2C). The two pollen chambers are confluent in the distal-most part of the anther (Figure S2D) and terminate in a single pore opening shortly before anthesis (Figure 2A). Mechanical compression of the appendage causes air contained in the intercellular spaces of the aerenchymatous tissue to surge through the connection zone of the appendage and pollen chambers (Figures 2C–2E). The resulting air current flushes the pollen grains through the apical anther pore (Figure 2F). Violent shaking, compressing the thecae, or applying vibrations with a tuning fork, mimicking vibrations occurring in buzz-pollination systems, where bees apply high-frequency vibrations to tubular anthers in order to shake out the pollen [4], could not expel noteworthy amounts of pollen from the anthers.

Comparison of stamen structure of closely related Melastomataceae species in the tribe Merianieae (*Graffenrieda cucullata* and *Meriania maxima* [bee pollinated], *Meriania sanguinea* [likely bat pollinated], and *Meriania pichinchensis* [bat pollinated]; Figures S1E-S1G) showed that stamen appendages in these species consist of densely packed parenchyma cells (Figures S2E–S2G).

Metabolomic Characterization of Stamen Appendages

We employed gas chromatography mass spectrometry of appendage material of *A. confusa* to assess the metabolome and nutritive value of the stamen appendages. The appendages were sugary, with high amounts of hexoses (fructose and glucose) (13.45 mg/g dry weight [dw], SD: 9.94 mg/g dw and 19.78 mg/g dw, SD: 9.05 mg/g dw, respectively), whereas sucrose was less abundant (7.00 mg/g dw, SD: 6.6 mg/g dw). Also, citric acid was abundant (9.96 mg/g dw, SD: 1.07 mg/g dw), and myo-Inositol (0.12 mg/g dw, SD: 0.06 mg/g dw) was also present (for a full list of detected metabolites, see Table S1). The energy content of the appendage tissue was 15,100 J/g dw (361.24 kCal/100 g dw).

Discussion

Pollination Mechanism and Mating System

Most Melastomataceae are buzz pollinated by bees [4], but bellows-like mechanisms have been reported in the few vertebrate-pollinated, nectariferous species [5, 6]. In rodent-pollinated *Blakea*, for example, copious nectar accumulates in the hypanthium [7]. By probing the flowers for nectar with their tongues, pollinating rodents push against the anthers and cause the expulsion of pollen clouds [6]. Whereas the pollen chambers themselves function as bellows-like structures in these Melastomataceae, the ejection of pollen is achieved

(G) *Iridosornis analis* (Tschudi, 1844) probing a flower of *A. confusa* and seizing a stamen.

(H) *Chlorospingus pileatus* (Salvin, 1864) holding a stamen of *A. costaricensis* by the appendage before swallowing it. Note the pollen grains on the bird's beak, front head, and cheeks. The photo is courtesy of Florian Etl.

The following abbreviations were used: hyp, hypanthium; se, sepals; pe, petals; f, filament; a, anther; app, appendage; g, gynoecium.

See also Figure S1 for comparison of other *Axinaea* species and closely related Melastomataceae from different genera in the tribe Merianieae. See Movie S1 for tanager feeding on *A. confusa* and activating the bellows mechanism.

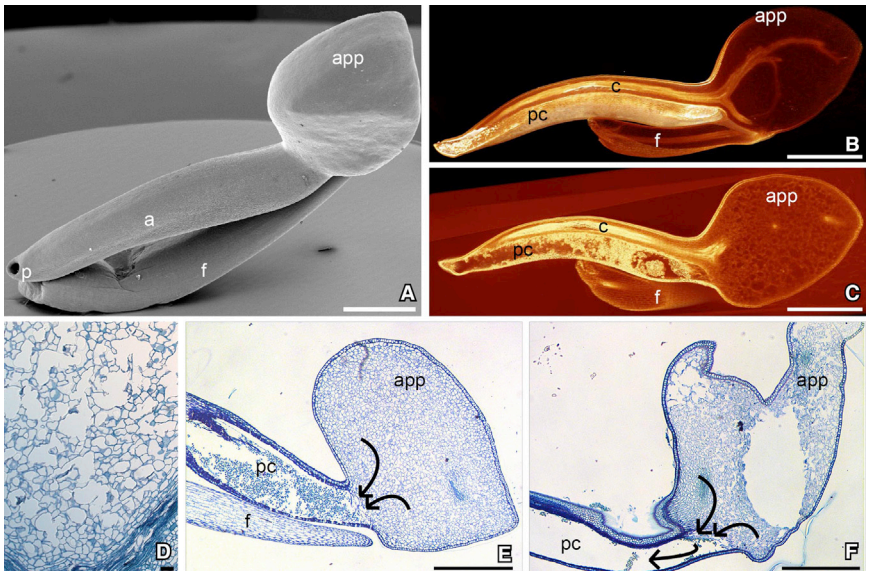

Figure 2. Detailed Stamen Morphology and Anatomy of *A. confusa*

(A) Scanning electron microscopy image of entire anthetic stamen. Note the proximity of the anther tip (pore) and filament base due to the folded structure of the stamen.

(B) Longitudinal section through anther based on a high-resolution X-ray computed tomographic (HRXCT) 3D reconstruction. Note the ramified vascular bundle in the appendage and the thick vascular strand within the connective tissue between the pollen chambers. Pollen chambers are clearly separated by cell layers from connective strand. Connective vascular strand does not have a function in the bellows mechanism.

(C) HRXCT image showing loosely packed aerenchymatic cells in appendage. Note the pollen visible in the pollen chamber. In this plane, the connection zone between appendage and base of pollen chamber starts to show.

(D–F) Light microscopic serial thin sections stained with ruthenium red and toluidine blue.

(D) Appendage aerenchyma with large intercellular spaces and partial vascular bundle (lower right).

(E) Longitudinal section of intact stamen. Arrows indicate direction of airflow when appendage is compressed. Note that there is no distinct cell layer separating appendage from pollen chambers and pollen contained in pollen chambers.

(F) Longitudinal section of stamen after artificial compression of appendage. Aerenchymatic tissue has been partly ruptured. Bellows can only be activated once. Arrows indicate airflow caused by compression of appendage. Note that most pollen has been flushed out of the pollen chamber.

The following abbreviations were used: a, anther; app, appendage; c, connective; f, filament; p, pore; pc, pollen chamber.

Scale bars of (A)–(C), (E), and (F) represent 1 mm. The scale bar of (D) represents 1 μm. See Figure S2 for structural comparison of Melastomataceae from different pollination syndromes. See Movie S3 for HRXCT scan of a stamen of *A. confusa*.

via the specialized aerenchymatous connective appendages in *Axinaea*, which are structurally separate and morphologically distinct from the pollen chambers. Also, the *Axinaea* bellows works only once per stamen, whereas it may be activated repeatedly in the bellows-like mechanisms of other Melastomataceae. As the birds remove stamens of *Axinaea* individually, functional repeatability of the mechanism is achieved by the independent provision of pollen by each stamen.

The structural comparison of stamen appendages of nectar-producing Merianieae confirms the uniqueness of the bellows structures in *Axinaea*. The appendages of *M. sanguinea* and *M. pichinchensis* do not differ notably from the buzz-pollinated *M. maxima* and *G. cucullata*. Renner [4] suggested that the diverse appendages found in Melastomataceae may function as handles for the buzzing bees; however, rigorous tests of this hypothesis are lacking.

Bellows-like mechanisms have been described for several *Solanum* species (*Cyphomandra*: Solanaceae) [8] in which euglossine bees cause pollen ejection when touching the thecae while collecting fragrance rewards. All known bellows and bellows-like mechanisms are characterized by poricidal anthers and belong to predominantly buzz-pollinated families. In contrast to buzz-pollination systems, bellows and bellows-like mechanisms appear to be correlated with the evolution of additional rewards (besides pollen), such as nectar (some Melastomataceae genera), food bodies (*Axinaea*), or fragrances (*Solanum*).

Because no other floral visitors capable of activating the bellows mechanism could be documented, we consider the tanagers and finches as legitimate pollinators of *Axinaea*. This conclusion is further supported by our observations of pollen deposition on the birds' heads, by the fact that the birds touch the stigmas while feeding (Figure 1G; Movie S2), and by Rojas-Nossa's [9] findings of tanagers carrying pollen of *A. macrophylla* (Colombia).

Axinaea relies on active pollen transfer, either via pollinating birds or directly via pollen clouds originating from within the same or neighboring flowers during the activation of the bellows mechanism by a bird (facilitated selfing [10]). Reproductive assurance may be guaranteed by the self-compatibility mechanism and by the fact that more than 50% of flowers are visited more than once, increasing chances of successful pollination.

Bird Pollination and Food Body Reward

The majority of bird pollinators visit flowers offering large quantities of nectar [11]. Despite controversial discussions of sugar preferences of hummingbirds and passerines, the classical model predicts that flowers visited by hummingbirds produce nectar rich in sucrose and that those visited by passerines offer nectar rich in hexoses [12, 13, 14]. The high concentration of hexoses (fructose and glucose) in the appendages of *A. confusa* conforms to this model [12]. Because the aerenchymatous appendage tissue did not show high cytoplasmic activity, we assume that the sugar reward is largely contained in the highly ramified vasculature (Figure 2B and Movie S3) and derived from sucrose-rich phloem sap converted to hexose by enzyme activity [14].

There are few documented cases of floral or extrafloral food body rewards in bird pollination, and these are all related to nonreproductive organs (glucose-rich corolla appendages [Calceolariaceae] [15]; edible bracts [Pandanaceae] [16]; deceit fruits [Araliaceae] [17]). In Myrtaceae (closely related to Melastomataceae), there are two known cases of pollination effected by tanagers feeding on petals of nectarless flowers [18, 19]. None of these studies characterize the metabolome or caloric value of the respective food bodies. However, with

Table 1. Floral Visitors of *Axinaea*

Axinaea Species	Bird Species	Family	Observations
A. confusa	yellow-throated tanager, *Iridosornis analis* (Tschudi, 1844)	Thraupidae	5 (222 hr of video monitoring)
	lacrimose mountain tanager, *Anisognathus lacrymosus* (Du Bus de Gisignies, 1846)	Thraupidae	1 (222 hr of video monitoring)
	blue-winged mountain tanager, *Anisognathus somptuosus* (Lesson, 1831)	Thraupidae	1 (direct observation)
	orange-bellied euphonia, *Euphonia xanthogaster* (Sundevall, 1834)	Fringillidae	1 (direct observation)
A. sclerophylla	masked flowerpiercer, *Diglossa cyanea* (Lafresnaye, 1840)	Thraupidae	1 (79 hr of video monitoring)
A. costaricensis	sooty-capped bush tanager, *Chlorospingus pileatus* (Salvin, 1864)	Thraupidae	1 (direct observation)

Single birds were recorded on *A. confusa* and *A. sclerophylla*, whereas tanagers foraged in groups of about five individuals on *A. costaricensis*. See Movie S2 for tanager removing stamens on *A. confusa* and contacting the stigma. See Table S1 for a list of metabolites contained in the appendage tissue of *A. confusa*.

approximately 15,100 J/g appendage tissue, the caloric value of *Axinaea* food bodies is comparable to caloric values of food bodies in beetle-pollinated Araceae [20] and of fruits of various tropical plant species [21]. Total caloric gain for the birds is likely even higher given the thick vascular bundle in the connective strand (Figures 2B and 2C; Movies S2 and S3) not included in our analyses. Because most tanagers feed on both fruits and insects, *Axinaea* food bodies may constitute a supplement to the birds' diet [22].

Evolutionary Framework

The center of diversity of *Axinaea* lies in the Andes of southern Ecuador and northern Peru, between 1,000 m and 3,600 m [23]. Because the exact phylogenetic relationships of *Axinaea* have not yet been established, it remains unclear whether passerine pollination originated directly from bee-pollinated ancestors or whether it is derived from nectariferous hummingbird-pollinated species, although the former appears to be more likely (D.S.P. et al., 2013, Botany Conference). Viewed from an evolutionary perspective, the pollination syndrome of *Axinaea* adds to Cruden's hypothesis [24] that bird pollination replaces bee pollination with increasing altitude because bees prove to be less-reliable pollinators under montane weather conditions. Within the mainly bee-pollinated Melastomataceae, a trend has been observed in which species with alternative pollination syndromes (bats, hummingbirds, rodents) occur at higher elevations [7]. Such shifts from bee to hummingbird pollination have been reported in other Andean flowering-plant genera [25, 26] and are correlated with the Andean uplift during the Miocene and the diversification of hummingbirds and mountain tanagers [27]. Whether these patterns also hold true for *Axinaea* remains to be investigated.

Conclusions

Interactions between plants and their pollinators include some of the most sophisticated and intriguing ecological and evolutionary relationships known to science. The novelty of the pollination syndrome of *Axinaea* lies in (1) having evolved a specialized bellows organ activated by the pollinator and in (2) providing highly nutritious food body reward on male reproductive organs. Also, this discovery opens up important trajectories for future research on pollinator-driven evolution in Neotropical Melastomataceae, specifically focusing on relationships of pollinator reward, pollinator type, mode of pollen deposition, and floral morphology.

Table 2. Fruit Sets in the Different Mating System Experiments

Treatment	Number of Fruits	Number of Flowers
Autogamy	15	90
Apomixis	0	88
Hand-self	67	95
Hand-cross	55	89
Natural	57	99

Experimental Procedures

Field Locations and Taxon Sampling

Collection of floral material was conducted in Ecuador (*A. confusa*, *A. sclerophylla*, *A. affinis*, *A. macrophylla*) and Costa Rica (*A. costaricensis*). For details, see Supplemental Experimental Procedures.

Video Monitoring of Floral Visitors

Video monitoring of floral visitors was carried out on *A. confusa* and *A. sclerophylla* (Podocarpus National Park, Ecuador; October 2012–December 2012). Two cameras were used to monitor floral visitors (06:00–18:00) for 214 hr and 79 hr, respectively. In addition, a total of 8 hr of night observations were made. The mating system of *A. confusa* was investigated with bagging experiments to assess apomixis, self-compatibility, and outcrossing. Stamen removal over the flowering period was monitored in 43 flowers of *A. confusa* by counting present stamens on mornings and evenings (control for night removal). Additionally, observations were made on *A. costaricensis* (Finca Truchas Selva Madre, Costa Rica; March 2014).

Birds were identified using Ridgely and Greenfield's field guide [28]. Classification follows the IOC World Bird List, version 3.5 [29].

Structural Analyses

Anthetic flowers and buds of five *Axinaea* and several Merianieae species were fixed in formaldehyde-acetic acid-alcohol (FAA). We employed light microscopy of sectioned stamens and scanning electron microscopy to study structural features. Furthermore, we carried out X-ray computed tomography of single stamens and entire flowers, prepared following the methods of Staedler et al. [30], to obtain high-resolution 3D images of the bulbous appendages for volume calculations (Amira 5.4.1). For details, see Supplemental Experimental Procedures.

Metabolomic Analyses

Appendage tissue (microwave shock dried, with filaments and thecae removed; 8–10 mg [31]; n = 9) was used for gas chromatography time-of-flight mass spectrometry. Absolute quantification of glucose, fructose, sucrose, citric acid, myo-Inositol, galactinol, and trehalose was obtained by measuring a standard mix. In order to determine the caloric content, we pooled (0.403 g) and analyzed microwave shock dried, pulverized tissue of several appendages in an IKA calorimeter. For details, see Supplemental Experimental Procedures [32, 33].

Supplemental Information

Supplemental Information includes Supplemental Experimental Procedures, two figures, one table, and three movies and can be found with this article online at http://dx.doi.org/10.1016/j.cub.2014.05.056.

Acknowledgments

We thank Konrad Fiedler, Jürgen Homeier, Xavier Clavijo, and the Estación Científica San Francisco for support with fieldwork in Ecuador. We are indebted to Anton Weissenhofer and Florian Etl for help with fieldwork in Costa Rica. We thank Ruth Quint for her assistance in the calorimetric

analyses. Furthermore, we thank Susanne Pamperl and Thomas Kreisberger for their support with tomographic analyses. This study was supported by grants to D.S.P. from the National Science Foundation (DEB-0508582 and DEB-1146409) and by a fellowship from the University of Vienna to A.S.D. The present study is integrated in the key research area "Patterns and Processes of Plant Evolution and Ecology" of the Faculty of Life Sciences at the University of Vienna.

Received: April 3, 2014
Revised: April 30, 2014
Accepted: May 22, 2014
Published: July 3, 2014

References

1. Armbruster, W.S. (2011). Evolution and implications of "specialized" pollinator-rewards. In Evolution of Plant-Pollinator Relationships, S. Patiny, ed. (Cambridge: Cambridge University Press), pp. 44–67.
2. Proctor, M.C.F., Yeo, P., and Lack, A. (1996). The Natural History of Pollination (Portland: Timber Press).
3. Simpson, B.B., and Neff, J.L. (1981). Floral rewards: alternatives to pollen and nectar. Ann. Mo. Bot. Gard. *68*, 301–322.
4. Renner, S.S. (1989). A survey of reproductive biology in Neotropical Melastomataceae and Memecylaceae. Ann. Mo. Bot. Gard. *76*, 496–518.
5. Vogel, S. (1997). Remarkable nectaries: structure, ecology, organophyletic perspectives I. Substitutive nectaries. Flora *192*, 305–333.
6. Lumer, C. (1980). Rodent pollination of *Blakea* (Melastomataceae) in a Costa Rican cloud forest. Brittonia *32*, 512–517.
7. Varassin, I.G., Penneys, D.S., and Michelangeli, F.A. (2008). Comparative anatomy and morphology of nectar-producing Melastomataceae. Ann. Bot. (Lond.) *102*, 899–909.
8. Sazima, M., Vogel, S., Cocucci, A.A., and Hausner, G. (1993). The perfume flowers of *Cyphomandra* (Solanaceae): pollination by euglossine bees, bellows mechanism, osmophores, and volatiles. Plant Syst. Evol. *187*, 51–88.
9. Rojas-Nossa, S.V. (2007). Estrategías de extracción de nectar por Pinchaflores (Aves: *Diglossa* y *Diglossopis*) y sus efectos sobre la polinización de plantas de los altos Ándes. Ornitología Colombiana *5*, 21–39.
10. Lloyd, D.G., and Schoen, D.J. (1992). Self- and cross-fertilization in plants. I. Functional dimensions. Int. J. Plant Sci. *153*, 358–369.
11. Cronk, Q., and Ojeda, I. (2008). Bird-pollinated flowers in an evolutionary and molecular context. J. Exp. Bot. *59*, 715–727.
12. Baker, H.G., Baker, I., and Hodges, S.A. (1998). Sugar composition of nectars and fruits consumed by birds and bats in the tropics and subtropics. Biotropica *30*, 559–586.
13. Nicolson, S.W., and Fleming, P.A. (2003). Nectar as food for birds: the physiological consequences of drinking dilute sugar solutions. Plant Syst. Evol. *238*, 139–153.
14. Nicolson, S.W., and Thornburg, R.W. (2007). Nectar chemistry. In Nectaries and Nectar, S.W. Nicolson, M. Nepi, and E. Pacini, eds. (Dordrecht: Springer), pp. 215–263.
15. Sérsic, A.N., and Cocucci, A.A. (1996). A remarkable case of ornithophily in *Calceolaria*: food bodies as rewards for a non-nectarivorous bird. Bot. Acta *109*, 172–176.
16. Porsch, O. (1923). Blütenstände als Vogelblumen. Österreichische Botanische Zeitschrift *72*, 125–149.
17. Pijl, L.d. (1961). Ecological aspects of flower evolution. II. Zoophilous flower classes. Evolution *15*, 44–59.
18. Roitman, G.G., Montaldo, N.H., and Medan, D. (1997). Pollination biology of *Myrrhinium atropurpureum* (Myrtaceae): sweet, fleshy petals attract frugivorous birds. Biotropica *29*, 162–168.
19. Sazima, I., and Sazima, M. (2007). Petiscos florais: pétalas de *Acca sellowiana* (Myrtaceae) como fonte alimentar para aves em área urbana no Sul do Brasil. Biota Neotropica *7*, 307–312.
20. Young, H.J. (1986). Beetle pollination of *Dieffenbachia longispatha* (Araceae). Am. J. Bot. *73*, 931–944.
21. Schaefer, H.M., Schmidt, V., and Wesenberg, J. (2002). Vertical stratification and caloric content of the standing fruit crop in a tropical lowland forest. Biotropica *34*, 244–253.
22. Snow, B.K., and Snow, D.W. (1971). The feeding ecology of tanagers and honeycreepers in Trinidad. Auk *88*, 291–322.
23. Balslev-Cotton, M.E. (2003). A taxonomic revision of the genus *Axinaea* Ruiz & Pav. (Melastomataceae). MSc thesis (Aarhus: University of Aarhus).
24. Cruden, R.W. (1972). Pollinators in high-elevation ecosystems: relative effectiveness of birds and bees. Science *176*, 1439–1440.
25. Kay, K.M., Reeves, P.A., Olmstead, R.G., and Schemske, D.W. (2005). Rapid speciation and the evolution of hummingbird pollination in neotropical Costus subgenus Costus (Costaceae): evidence from nrDNA ITS and ETS sequences. Am. J. Bot. *92*, 1899–1910.
26. Smith, S.D., Ané, C., and Baum, D.A. (2008). The role of pollinator shifts in the floral diversification of *Iochroma* (Solanaceae). Evolution *62*, 793–806.
27. Barker, F.K., Burns, K.J., Klicka, J., Lanyon, S.M., and Lovette, I.J. (2013). Going to extremes: contrasting rates of diversification in a recent radiation of new world passerine birds. Syst. Biol. *62*, 298–320.
28. Ridgely, R.S., and Greenfield, P.J. (2001). The Birds of Ecuador: Field Guide (Ithaca: Cornell University Press).
29. Gill, F., and Donsker, D. (2013). IOC World Bird List, Version 3.5. http://worldbirdnames.org/updates/.
30. Staedler, Y.M., Masson, D., and Schönenberger, J. (2013). Plant tissues in 3D via X-ray tomography: simple contrasting methods allow high resolution imaging. PLoS ONE *8*, e75295.
31. Popp, M., Lied, W., Meyer, A.J., Richter, A., Schiller, P., and Schwitte, H. (1996). Sample preservation for determination of organic compounds: microwave versus freeze-drying. J. Exp. Bot. *47*, 1469–1473.
32. Weckwerth, W., Wenzel, K., and Fiehn, O. (2004). Process for the integrated extraction, identification and quantification of metabolites, proteins and RNA to reveal their co-regulation in biochemical networks. Proteomics *4*, 78–83.
33. Furuhashi, T., and Weckwerth, W. (2013). Introduction to lipid (FAME) analysis in algae using gas chromatography-mass spectrometry. In The Handbook of Plant Metabolomics, W. Weckwerth and G. Kahl, eds. (Weinheim: Wiley), pp. 215–225.

Current Biology, Volume *24*

Supplemental Information

A Specialized Bird Pollination System with a Bellows Mechanism for Pollen Transfer and Staminal Food Body Rewards

Agnes S. Dellinger, Darin S. Penneys, Yannick M. Staedler, Lena Fragner, Wolfram Weckwerth, and Jürg Schönenberger

Supplemental Data

Figure S1. Flowers of *Axinaea* and closely related Merianieae. (A), (B) *Axinaea affinis*, virgin anthetic flower (A) and flower after stamen removal (B); note more pronounced filament curvature in comparison to Figure 1A, B, D, E, resulting in distinct monosymmetric pattern of stamen arrangement. (C) *A. macrophylla*, stamens partially removed. (D) *A. sclerophylla*, a virgin flower and flower with only partial filaments remaining; note weighing of stamens to abaxial side of flower. (E) Flowers of buzz-pollinated *Graffenrieda cucullata* and (F) *Meriania maxima* with typical rotate corollas. (G) Flowers of presumably nectar producing and vertebrate pollinated *M. sanguinea* with pseudo-tubular corolla. (H) Flower of bat pollinated *M. pichinchensis* also with pseudo-tubular corolla.

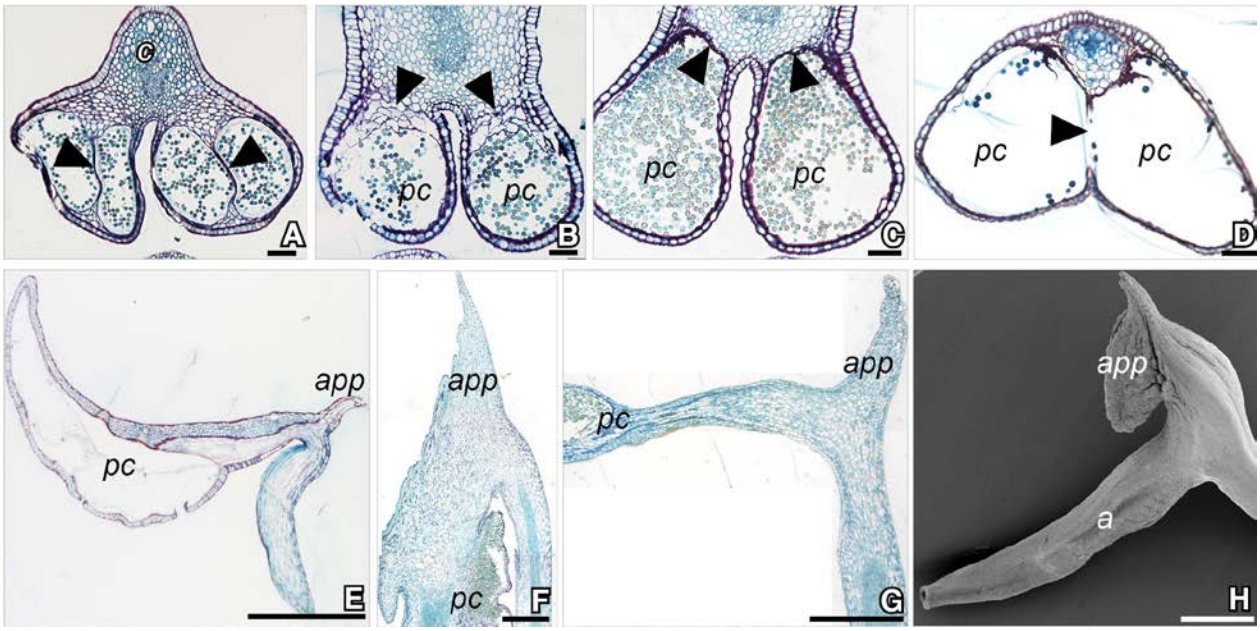

Figure S2. Detailed stamen anatomy of *Axinaea* and closely related Merianieae. (A) – (D) *A*. *confusa*, cross-sections of anthers. (A) Immature anther with septum separating pollen sacs. (B) Mature anther, section at connection zone of appendage and pollen–chamber, septa between pollen sacs have collapsed, arrowheads indicate areas where air enters pollen chambers; note absence of any tissue separating pollen-chamber from appendage aerenchyma (compare Figure 2E, F). (C) Section in the middle of anther, pollen chambers well separated from connective tissues by darker stained cell layers (arrowheads). (D) Section at tip of anther, pollen chambers confluent (arrowhead). (E) *Graffenrieda cucullata*, longitudinal section, tiny appendage and large pollen chamber. (F) *Meriania maxima*, longitudinal section of stamen, large subulate appendage and proximal part of theca. (G) *M. pichinchensis*, note elongated connective. (H) SEM image of *M. sanguinea*, connective appendage and sturdy anther. *a* = anther; *app* = appendage; *pc* = pollen chamber. Scale bar = 100 µm in A-D, 1 mm in E-H.

Table S1. Full list of metabolites of *Axinaea confusa* food bodies from metabolomic analyses. These metabolites were detected in the polar phase of the split 25-measurements; absolutely quantified metabolites (hexose, glucose, fructose, myo-Inositol, citric acid, galactinol and trehalose) are not included. Given values are peak areas normalized to the sum of all peaks of a chromatogram.

Metabolites	Sample 1	Sample 2	Sample 3	Sample 4	Sample 5	Sample 6	Sample 7	Sample 8	Sample 9
2,3-Dihydroxybutanedioic acid	0,009618	0,016072	0,019604	0,017854	0,017420	0,047648	0,019943	0,079441	0,010024
3-Hydroxy-3-methylglutaric acid	0,000070	0,000145	0,000185	0,000116	0,000116	0,000135	0,000214	0,000208	0,000108
4-Aminobutyric acid	0,032476	0,010511	0,022768	0,028201	0,025019	0,043470	0,023586	0,030808	0,010230
4-Hydroxy-L-Proline	0,000000	0,000865	0,001249	0,002253	0,001881	0,003541	0,002245	0,002161	0,000450
Alanine	0,006735	0,002903	0,024838	0,022028	0,022378	0,025816	0,007013	0,023599	0,007431
Aldohexose RI 2181	0,009452	0,012082	0,027024	0,106519	0,149472	0,078090	0,111542	0,036690	0,043821
Aldohexose RI2265	0,001436	0,000906	0,001368	0,001193	0,000918	0,001297	0,000668	0,001011	0,001076
Aspartic acid	0,001296	0,002042	0,001336	0,003863	0,009180	0,004850	0,002377	0,002527	0,000989
beta-Alanine	0,000671	0,000206	0,000725	0,000747	0,000653	0,000392	0,000214	0,000276	0,000132
Carbohydrate RI 2186	0,002252	0,002512	0,004325	0,003117	0,005099	0,012122	0,002974	0,003052	0,001305
Carbohydrate RI1838	0,146694	0,103048	0,049370	0,049290	0,042360	0,030104	0,060688	0,066322	0,087496
Carbohydrate RI1847	0,057139	0,081486	0,099313	0,086670	0,059461	0,053652	0,081877	0,105675	0,049001
Carbohydrate RI1853	0,149624	0,180973	0,173165	0,198095	0,175293	0,189417	0,123840	0,226500	0,139882
Carbohydrate RI1886	0,061251	0,045832	0,014989	0,016671	0,010103	0,013099	0,021135	0,025561	0,031103
Carbohydrate RI2071	0,026665	0,048006	0,021911	0,031003	0,008932	0,016692	0,038545	0,026359	0,009250
Carbohydrate RI2084	0,036286	0,053689	0,026210	0,043794	0,013280	0,032956	0,054348	0,036978	0,014982
Carbohydrate RI2168	0,000000	0,000537	0,000231	0,000259	0,000189	0,000229	0,000502	0,000304	0,000090
Carbohydrate RI3001	0,000322	0,000445	0,000404	0,000316	0,000352	0,000507	0,000369	0,001205	0,000193
Carbohydtrate RI1876	0,090844	0,049530	0,040032	0,015451	0,020724	0,006664	0,007904	0,018091	0,036412
Erythritol	0,037517	0,013871	0,011849	0,006820	0,022401	0,011659	0,010895	0,015539	0,040837
Erythronic acid	0,000698	0,000378	0,000311	0,000311	0,000952	0,000270	0,000402	0,000450	0,000617
Ethanolamine	0,009642	0,005525	0,008550	0,006124	0,006613	0,004700	0,002351	0,002081	0,001354
Fucose/Rhamnose	0,000679	0,000313	0,000392	0,000456	0,000678	0,000000	0,000871	0,000456	0,000345
Fumaric acid	0,003382	0,001013	0,001294	0,001568	0,002317	0,001551	0,000467	0,000969	0,001001
Fumaric acid, 2-methyl-	0,000170	0,000039	0,000099	0,000109	0,000127	0,000000	0,000292	0,000121	0,000000

Glutamic acid	0,000000	0,000000	0,000095	0,000300	0,000372	0,002207	0,000396	0,000440	0,000053
Glyceric acid	0,003058	0,001697	0,001984	0,001333	0,002355	0,001184	0,001448	0,000792	0,001427
Glycerol	0,016307	0,009832	0,010468	0,005546	0,014084	0,007550	0,002894	0,028096	0,387194
Glycine	0,001030	0,000981	0,003390	0,001830	0,001437	0,000782	0,000391	0,000480	0,000430
Glycolic acid	0,003123	0,000909	0,001035	0,000859	0,001149	0,001600	0,001454	0,000887	0,000625
Hexonic acid 1	0,011747	0,085233	0,046964	0,016938	0,020081	0,040714	0,071208	0,059191	0,025299
Hexonic acid 2	0,000154	0,000470	0,000492	0,000594	0,000429	0,001075	0,001093	0,001032	0,000492
Hexonic acid 3	0,000000	0,000175	0,000161	0,000276	0,000271	0,000393	0,000267	0,000722	0,000000
Ketohexose RI1677	0,001030	0,001282	0,001908	0,001206	0,002020	0,001399	0,002140	0,000795	0,000668
Ketohexose RI1686	0,003917	0,005886	0,008826	0,005197	0,009678	0,006007	0,010116	0,003666	0,002937
Ketohexose RI1692	0,003344	0,002286	0,003891	0,003401	0,003092	0,000636	0,001370	0,001047	0,002980
Ketohexose RI1707	0,011193	0,005036	0,007019	0,003737	0,006009	0,005276	0,005611	0,005597	0,010150
Leucine	0,001104	0,000518	0,003112	0,001229	0,002066	0,000208	0,000318	0,000356	0,000123
Lumichrome (7,8-Dimethylalloxazine)	0,001696	0,001169	0,001570	0,001107	0,001872	0,009007	0,001324	0,000881	0,001789
Maleic acid	0,000425	0,000052	0,000089	0,000224	0,000354	0,000000	0,000852	0,000121	0,000056
Malic acid	0,028106	0,017707	0,021508	0,052210	0,034111	0,034782	0,068584	0,012619	0,006829
NA RI 1448	0,106191	0,131547	0,198883	0,135588	0,130720	0,158334	0,088837	0,073163	0,014287
NA RI 1489	0,003752	0,002541	0,007822	0,005167	0,006985	0,005091	0,004431	0,005065	0,004291
NA RI 1772	0,001413	0,000673	0,000808	0,001938	0,001160	0,001739	0,000935	0,000779	0,000339
NA RI 2018	0,001310	0,001458	0,001317	0,000674	0,000000	0,000000	0,000139	0,000000	0,000706
NA RI 2331	0,000103	0,000126	0,000088	0,000289	0,000126	0,000335	0,000888	0,000726	0,000377
NA RI 2359	0,000193	0,000388	0,000356	0,000171	0,000469	0,000645	0,000549	0,000891	0,001802
NA RI 2417 (Sugar acid)	0,000367	0,000484	0,000548	0,000695	0,000643	0,000387	0,000649	0,000752	0,000271
NA RI1408	0,002115	0,001735	0,002131	0,001566	0,001601	0,001333	0,000571	0,000928	0,000777
NA RI1552	0,000355	0,000356	0,000430	0,001067	0,000338	0,000627	0,000295	0,000245	0,000207
Pentonic acid P1	0,000081	0,000259	0,000379	0,000479	0,000365	0,002033	0,001624	0,001237	0,000563
Pentonic acid P2	0,001117	0,000391	0,001020	0,001237	0,000856	0,001093	0,001214	0,000763	0,000496
Pentonic acid P3	0,000241	0,000173	0,000161	0,000258	0,000151	0,000000	0,000101	0,000159	0,000061
Phenylalanine	0,000323	0,000148	0,000704	0,000575	0,000457	0,000000	0,000398	0,000239	0,000102
Phosphoric acid	0,023495	0,000000	0,000000	0,000000	0,000000	0,006629	0,002976	0,000000	0,000000

Proline	0,001330	0,001191	0,004193	0,002865	0,002388	0,011319	0,000979	0,011677	0,000687
Pyroglutamic acid	0,018643	0,018182	0,027356	0,027576	0,045623	0,020058	0,012238	0,015915	0,012016
Pyruvic acid	0,000035	0,000029	0,000042	0,000040	0,000000	0,000000	0,000129	0,000086	0,000067
Quinic acid	0,000000	0,002459	0,001795	0,001733	0,001654	0,002197	0,002136	0,002798	0,000000
Raffinose	0,000000	0,000000	0,000000	0,000000	0,000000	0,000000	0,001009	0,000559	0,000257
Sedoheptulose, 2,7-anhydro-, beta-	0,007449	0,015100	0,011609	0,011442	0,012482	0,031037	0,032884	0,010690	0,000000
Serine	0,005050	0,002334	0,005550	0,004086	0,008958	0,007367	0,004165	0,004797	0,001251
Shikimic acid	0,031516	0,034572	0,036155	0,035367	0,055842	0,039631	0,069300	0,022545	0,019430
Succinic acid	0,006110	0,003164	0,005552	0,008395	0,004666	0,006118	0,001335	0,002345	0,000802
Threitol	0,000415	0,000315	0,000354	0,000273	0,000507	0,000378	0,000259	0,000307	0,000742
Threonic acid	0,007069	0,007750	0,010900	0,008784	0,010727	0,009030	0,020783	0,013347	0,007878
Threonic acid-1,4-lactone	0,000408	0,000327	0,000220	0,000218	0,000365	0,000708	0,000746	0,000393	0,000254
Threonine, allo-	0,001827	0,000435	0,001207	0,000782	0,001617	0,000935	0,000634	0,001391	0,000469
Threose/Erythrose	0,000000	0,000000	0,000000	0,000070	0,000000	0,000000	0,000105	0,000054	0,000167
Tryptophan	0,000000	0,000000	0,000254	0,000296	0,000328	0,000000	0,000400	0,001319	0,000000
Urea	0,000202	0,004887	0,009945	0,005404	0,007718	0,000593	0,000474	0,000415	0,000096
Valine	0,004725	0,001173	0,006165	0,002172	0,005023	0,000700	0,001221	0,001477	0,000724

Supplemental Experimental Procedures

TAXON SAMPLING

Collection of floral material was conducted in Ecuador and Costa Rica. In the Podocarpus National Park, Loja Province, Ecuador, we collected flowers and buds from a population of ca. 60 flowering individuals of *Axinaea confusa* E. Cotton & Borchs. (1800 – 2000 m; coll. no.: *Dellinger 10*), and from a population of ca. 15 individuals of *A. sclerophylla* Triana (2600 m, *Dellinger 24*). We collected floral material of two more species in Ecuador: *A. affinis* Cogn., in the Bosque Cristal, Azuay Province (3500 m; *Dellinger 42*), and *A. macrophylla* (Naudin) Triana in the Morona-Santiago Province between Gualaceo and Limon (2400 m) (*Penneys 1598*). In Costa Rica, we collected floral material of *A. costaricensis* Cogn. at the Finca Truchas Selva Madre, San José Province, at 3000 m (*Schönenberger 937*).Herbarium vouchers of *Axinaea confusa* and *A. sclerophylla* have been deposited in the herbarium of the Universidad Técnica Particular de Loja (UTPL), *A. affinis* in the herbarium of the Universidad del Azuay (HA); *A. costaricensis* in the herbarium of the University of Vienna (WU), and *A. macrophylla* in the University of Florida herbarium (FLAS).

For a detailed comparison of stamen structure and function of taxa closely related to *Axinaea*, we also collected floral material of *Meriania* and *Graffenrieda* in Ecuador: The buzz-pollinated *M. maxima* Markgr (*Penneys 1618*) and the hummingbird and bat-pollinated *M. pichinchensis* Wurdack (*Penneys 1905* [S1]) were collected in the Pichincha Province, *M. sanguinea* Wurdack, which resembles nectar secreting species in its overall floral shape, (*Dellinger 2*) was collected in the Podocarpus National Park, Ecuador; finally, *Graffenrieda cucullata* (Triana) L.O. Williams (*Penneys 1873*), another buzz-pollinated species, was sampled in the Esmeraldas Province, Ecuador.

Herbarium vouchers of *M. maxima*, *M. pichinchensis* and *Graffenrieda cucullata* are deposited at the University of Florida herbarium (FLAS) and specimens of *M. sanguinea* at the herbarium of the Technical University of Loja, Ecuador (UTPL).

VIDEO MONITORING OF FLORAL VISITORS IN THE FIELD

Video monitoring of floral visitors was carried out for populations of *Axinaea confusa* and *A. sclerophylla* in the Podocarpus National Park, Ecuador from October to December 2012. The population of *A. confusa* consisted of ca. 60 individuals, and was found in secondary forest and open grassland at elevations of 1800 m to 2200 m. The population of *A*. *sclerophylla* was found along an abandoned road at 2600 m to 2700 m. Two cameras (Sony HDR-CX 190) were used to monitor floral visitors during the day (6:00 – 18:00) for 214 and 79 hours over a period of four

and two weeks, respectively. The cameras were stationed at inflorescences with at least one freshly opened flower. Documented visits would therefore not conform to overall visitation of the plant as cameras were focused to film one to a few inflorescences on trees bearing hundreds of inflorescences. Flowers were observed on four nights (20:00 – 22:00) for possible nocturnal visitors.
Additionally, direct observations were made on *A*. *costaricensis* at Finca Truchas Selva Madre, Costa Rica, in March 2014.
The birds were identified using Ridgely & Greenfield's field guide [28], classification follows the IOC World Bird List 3.5 [29].

In order to detect a pattern in the removal of stamens, 43 virgin flowers of *A. confusa* were tagged on their first morning of flowering (ten stamens present). The flowers were monitored at dawn every following morning and number of present stamens was recorded until all ten stamens had been removed. In 20 of these 43 flowers, the number of stamens was also checked at dusk to control for possible stamen removal during the night.

To study the mating system of *A*. *confusa*, entire inflorescences were bagged with bridal veil to exclude floral visitors, marked with jeweller's paper tags and five different treatments were applied: (1) autogamy – inflorescences bagged at pre-anthesis and left untouched, (2) – apomixis – stigmas were removed or flowers were emasculated, (3) hand self-pollination – pollen was transferred manually within the emasculated flower, (4) hand cross-pollination – pollen from a different individual was transferred to the stigma of the emasculated flower, (5) open pollination – single tagged flowers were exposed to natural pollination. Tweezers were used to manually transfer pollen to stigmas and cleaned with 96% ethanol between trials. The experimental inflorescences were checked every one to three days, the abortion of flowers and fruits was noted and after four to six weeks, the fruit set of all treatments was recorded. Fruit-set in autogamy trials may have been caused by our manipulative experiments when pollen clouds ejected from neighbouring flowers reached stigmas of autogamy-trial flowers. A self-compatibility index (SCI) was calculated and a ratio < 0.2 was considered self-incompatible [S2]. Comparison of fruit-set in experiments (4) and (5) provide an indication of pollen limitation [S3]. To assess the risk of self-pollination, pollen deposition following pollen ejection from the anthers was analysed. In virgin flowers, all ten appendages were squeezed with tweezers to cause pollen expulsion. In a subset of 10 flowers, the presence of pollen on stigmas was checked using a light microscope. In the remaining 90 flowers, the resulting fruit set was recorded after two to four weeks. X^2-tests were calculated to test for differences in fruit sets using R (R Developmental Core Team 2011).

STRUCTURAL ANALYSIS - DETAILS

Anthetic flowers and floral buds in different developmental stages were fixed in FAA (Formaldehyde-Acetic acid-Alcohol) and subsequently transferred to 70% ethanol.

For thin sectioning and light microscopy, single stamens (with appendage either intact or compressed) were extracted from mature buds, infiltrated (Technovit 7100, hardener I, Heraeus Kulzer, Wehrheim, Germany) and embedded in 2-hydroxyethyl methacrylate (Technovit 7100, hardener II). Transverse and longitudinal serial sections of 6-7 µm thickness were prepared using a Microm HM rotary microtome 355 (Walldorf, Germany) and sections were stained with 0.2% – Ruthenium red – 0.5% – Toluidine (RT-stain) [S4]. Permanently mounted slides (Histomount; National Diagnostics, Atlanta, GA, USA) are deposited in the Department of Botany and Biodiversity Research in Vienna. Digital images of selected sections were taken with a Nikon digital sight DS-Fi1 camera (Nikon Corporation, Tokyo, Japan) on an Olympus BX50 system microscope (Olympus Optical Corporation, Tokyo, Japan).

Scanning Electron Microscopy (SEM) was used to observe mature stamens and the inner hypanthium wall of all five species of *Axinaea* to screen for possible nectar releasing structures. Samples were dehydrated over an ethanol series, critical point dried (CP Autosamdri-815), coated with gold using a Sputter Coater (SCD 050), then mounted onto aluminium stubs and scanned in a JEOL JSM-6390 at 10 kV.

For High Resolution X-Ray Computed Tomography (HRXCT), floral samples of *A. confusa* were infiltrated with 1% PTA (Phosphotungstic acid) – 70% Ethanol for a week in order to increase contrast. The PTA solution was changed daily. Samples were then dehydrated in 1% PTA – 96% Ethanol, transferred to acetone, CP-dried and mounted for HRXCT in an Xradia MicroXCT-200 system (http://www.xradia.com; Pleasanton, CA, USA) [5 separate scans for complete object; source settings: 55 kV, 44 µA; optical magnification: 10.042; binning: 1; exposure time: 10 s; number of exposures: 728; pixel size: 1.04 µm]. Detailed descriptions of sample preparation are given in Staedler et al. [30]. For volume calculation (cells vs. intercellular spaces in appendages), a 3D reconstruction was performed (XMReconstructor XRadia Inc.) and the five scans were stitched together, filtered in XMR-Controller to increase contrasts and calculations were carried out in the programme Amira 5.4.1 (Visualization Sciences Group, SAS, http://www.visageimaging.com). To calculate total intercellular space, conservative grayscale thresholds were chosen (0-12500) in order to avoid overestimation.

METABOLOMIC ANALYSIS - DETAILS

Single stamens of *Axinaea confusa* were microwave-shock-dried (2:50 minutes at 600 watt) and afterwards dried properly in a drying closet overnight at 40°C [31]. Filaments and anthers were removed prior to pulverization of the material so that only the appendage content was present in the sample. We did this to avoid misleading results by measuring pollen (rich in energy and proteins) still present in the thecae of undamaged stamens.

For each sample, 8 - 10 µg of the pulverized tissue from 8 - 15 appendages of nine independent plant individuals (n = 9) were used and extracted following a protocol from Weckwerth et al. [32]. After separation of the apolar and polar phase each phase was separated into two equal aliquots before drying in a vacuum centrifuge (Scan Vac). Dried extracts were used to analyse polar and apolar compounds as their trimethylsilyl esthers by GC-TOF-MS (LECO Pegasus® 4D GCxGC-TOFMS Instrument (Mönchengladbach, Germany) [32]. Fatty acids were analysed as their methylesthers (FAME) according to [33] using GC-MS (Thermofisher Scientific TSQ Quantum GC™, Bremen, Germany). Derivatised polar phase was measured two times (i) diluted 1:75 with pyridine prior to split less injection (SL) and (ii) undiluted with a split ratio of 1:25 (S25, split injection). Derivatised apolar phase was injected split less. For absolute quantification of glucose, fructose, sucrose, citric acid, myo-inositol, galactinol and trehalose, a standard mix was measured in different concentrations before, between and after the samples for external calibration. Baseline substraction, peak detection and library search was performed with the instruments vendor's software ChromaTof® (Leco). Identification was based on mass spectral matches (>850) and maximum retention index deviation of 70 compared to an in-house mass spectral library. Peak areas were used for relative quantification. Calibration curves for absolute quantification of diluted samples (1:75) were calculated in Excel (Office 2010, Microsoft). Significant amounts of some polar metabolites were also found in the apolar phase. For correction of absolute values, quantified amounts of polar and apolar phase were summed. Mean values and standard deviations were calculated from 9 independent biological replicates.

In order to determine the caloric content of the food bodies, connective appendages were prepared as described above for the GC-MS. The samples of the nine individuals had to be pooled to have sufficient material for the analysis. 0.403 g of the pulverized material was compressed into a pellet and analysed in an IKA calorimeter C 2000 basic Version 1 (IKA®-Werke GmbH & Co. KG, Germany).

Supplemental References

S1. Muchhala, N. (2002). Flower visitation by bats in cloud forests of western Ecuador. *Biotropica 34*, 387-395.

S2. Etcheverry, A.V., Alemán, M.M. and Fleming, T.F. (2008). Flower morphology, pollination biology and mating system of the complex flower of *Vigna caracalla* (Fabaceae: Papilionoideae). Ann. Bot. *102*, 305-316.

S3. DeWaal, C., Anderson, B. and Barrett, S.C.H. (2012). The natural history of pollination and mating in bird-pollinated *Babiana* (Iridaceae). Ann. Bot. *109*, 667-679.

S4. Ruzin, S.E. (1999). Plant Microtechnique and Microscopy (New York: Oxford University Press).